



2/3 octave Si/SiO₂ infrared dispersive mirrors open new horizons in ultrafast multilayer optics

VLADIMIR PERVAK,^{1,*} TATIANA AMOTCHKINA,^{1,2} QING WANG,^{2,3} OLEG PRONIN,¹ KA FAI MAK,² AND MICHAEL TRUBETSKOV²

¹Ludwig-Maximilians-Universität München, Am Coulombwall 1 85748 Garching, Germany

²Max-Planck-Institut für Quantenoptik, Hans-Kopfermann-Str. 1 85748 Garching, Germany

³School of Optics and Photonics, Beijing Institute of Technology 100081 Beijing, China

*Vladimir.Pervak@lmu.de

Abstract: Dispersive mirrors operating in a broadband infrared spectral range are reported for the first time. The mirrors are based on Si/SiO₂ thin-film materials. The coatings exhibit reflectance exceeding 99.6% in the spectral range from 2 to 3.2 μm and provide a group delay dispersion of −100 fs² and −200 fs² in this range. The fabricated mirrors are expected to be key elements of Cr:ZnS/Cr:ZnSe femtosecond lasers and amplifiers. The mirrors open a new avenue in the development of ultrafast dispersive optics operating in the infrared spectral range.

© 2019 Optical Society of America under the terms of the [OSA Open Access Publishing Agreement](#)

1. Introduction

Over the last twenty years broadband dispersive mirrors (DM) have become key optical components in modern laser systems [1–5]. Dispersive multilayer components provide efficient help to amplify, drive, and shape laser pulses. Until now, DMs operate effectively in the systems based on Ti:Sa lasers (~800 nm) and near-infrared Yb:YAG lasers (~1030 nm). The DM technology is becoming more widespread for Thulium- and Holmium-based laser systems operating around 1.9–2.2 μm [6,7]. The developing laser technology based on 2.4 μm chromium doped zinc sulfide (Cr:ZnS) will extend laser output to 3.2 μm [8,9]. The main prerequisite for development of this technology is availability of dispersive optics covering the entire spectral range from 2 to 3.2 μm. The latest and the best achievements in this direction is a DM operating in the range 2.2–2.7 μm (one-third of an octave only) with the group delay dispersion (GDD) of −200 fs² and a high-reflector compensating the third-order dispersion of −3000 fs³ [10]. These optical elements do not cover the broadband spectral range of interest. The ground motivation of the present work is to push frontiers in the cutting edge of the laser technology and to make a large step forward towards development of laser optics for 2–4 μm region. The DMs presented in the present work exhibit reflectance exceeding 99.6% and GDD values of (−100 fs²) and (−200 fs²). The DMs cover the range from 2 to 3.2 μm, i.e. span two thirds of an octave. Importantly, in the wavelength range between 2.7 μm and 2.9 μm, where OH-absorption would be expected, the mirrors exhibit almost no degradation of reflectance.

A choice of thin-film materials for 2–4 μm dispersive optics is a challenge since layer materials typically used in the visible-near-infrared ranges provide the refractive index ratios, which are not enough to achieve both high reflectance, and specified GDD values in the broad infrared spectral ranges. In [2], a 50-layer DM operating in the spectral range from 2.5 to 2.4 μm and providing GDD of + 3000 fs² was reported. The DM consists of Nb₂O₅ and SiO₂ layers and has physical thickness of 41 μm. The use of the same material pair Nb₂O₅/SiO₂ or other pairs typical for the visible-near-infrared ranges such as Ta₂O₅/SiO₂, TiO₂/SiO₂ cannot provide target negative GDD values required for the development of Cr:ZnS oscillator since

inevitable oscillations in GDD [11] reach too high values. In the present work, the thin-film materials Si and SiO₂ are used for the first time for the design and production of DMs in the infrared spectral range from 2 to 3.2 μm.

In Section 2, design and production of the DMs are described. In Section 3, experimental data are presented and discussed. Conclusions are presented in Section 4.

2. Design and production

For the DMs operating in the range 2-3.2 μm, the pair thin-film materials Si/SiO₂ is very promising since a quite high ratio of the refractive index values (≈ 2.3) is provided. For comparison, thin-film materials typically used in the visible-near-infrared spectral ranges have the refractive index ratio 1.4-1.6. As a substrate, Suprasil (fused silica) of 6.35 mm thickness was used. *Nominal* refractive indices of SiO₂ and Suprasil were described by the well-known Cauchy formula:

$$n(\lambda) = A_0 + A_1 \left(\frac{\lambda_0}{\lambda} \right)^2 + A_2 \left(\frac{\lambda_0}{\lambda} \right)^4, \quad (1)$$

where A_0, A_1, A_2 are dimensionless parameters, $\lambda_0 = 1000$ nm, λ is specified in nanometers. For SiO₂ $A_0 = 2.065721$, $A_1 = 0.016830$, $A_2 = 0.001686$, and for Suprasil $A_0 = 1.443268$, $A_1 = 0.00406$, $A_2 = 6.948 \cdot 10^{-6}$. The dispersion data of Si layers was found in the following way. As a first approximation, Si refractive index values were taken from [12]. The wavelength dependence $n_H(\lambda)$ can be approximated in the spectral range from 1400 nm to 5000 nm by the Cauchy formula with $A_0 = 3.413463$, $A_1 = 0.150903$, $A_2 = -3.305936 \cdot 10^{-3}$.

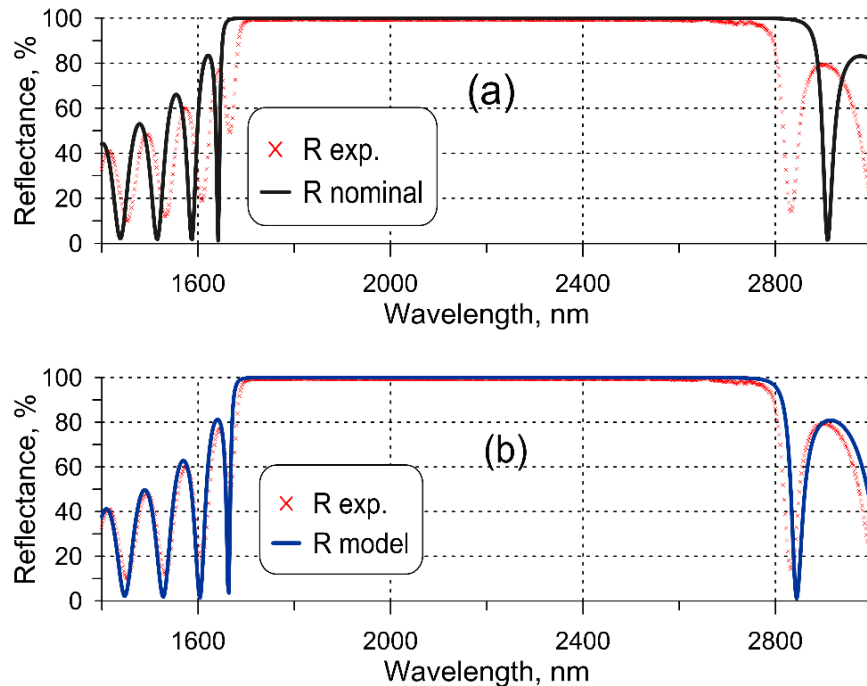


Fig. 1. (a) Initial correspondence between experimental and nominal reflectance data; (b) Correspondence between experimental and model reflectance data after indices correction. The data are related to the 13-layer quarter-wave mirror.

A 13-layer quarter-wave mirror with the central wavelength of 2100 nm was fabricated. Reflectance data of the produced quarter-wave mirror was measured with the help of Universal Reflectance accessory (Perkin Elmer) in the range from 1400 nm to 3000 nm where Si-layers are definitely non-absorbing. The initial correspondence between nominal and experimental data is shown in Fig. 1(a). In this Figure, one can easily observe that the high reflection zone of the produced sample is narrower than the width of the high reflection zone predicted by the theory. It follows from the estimation of the width of the high reflection zone ([13], p. 77) that the actual ratio of the high and low refractive index values is smaller than the ratio of the nominal refractive indices. Hence, it can be assumed that the Si-refractive-index has a negative offset, i.e. actual refractive index is $n_H(\lambda) - \Delta n_H$ instead of $n_H(\lambda)$. Calculating model reflectance for different values of this offset Δn_H , it is possible to find the best correspondence between the measurement and model reflectance data (see Fig. 1(b)). The best fitting is achieved with $\Delta n_H = 0.2$. For further theoretical designing, the Si-refractive index was described by the Cauchy formula with $A_0 = 3.213463$, $A_1 = 0.150903$, $A_2 = -3.305936 \cdot 10^{-3}$.

The DM designs were calculated with the help of the needle optimization method implemented into the OptiLayer software [14,15]. The design process was based on the optimization of the merit function evaluating the closeness of actual and target spectral characteristics. The merit function was defined as

$$MF^2 = \sum_{j=1}^{500} \left(\frac{R^{(p)}(\mathbf{X}; \lambda_j) - \hat{R}(\lambda_j)}{\Delta_{1,j}} \right)^2 + \sum_{j=1}^{500} \left(\frac{GDD^{(p)}(\mathbf{X}; \lambda_j) + G\hat{D}D(\lambda_j)}{\Delta_{2,j}} \right)^2, \quad (2)$$

where $\{\lambda_j\}$ are evenly distributed wavelength points in the spectral range of interest from 2000 nm to 3200 nm, $\mathbf{X} = \{d_1, \dots, d_m\}$ is the vector of layer thicknesses, m is the number of layers, $\{\Delta_{1,j}\}$ [%] and $\{\Delta_{2,j}\}$ [fs²] are design tolerances, the angle of incidence is 5°, (p) denotes p -polarization. In Eq. (2), \hat{R} and $G\hat{D}D$ are target reflectance and target GDD, respectively.

In the present work, two design problems were solved. In both design problems, target reflectance was 100% (that corresponds to the first term in Eq. (2)). Target group delay dispersion $G\hat{D}D$ equals to -100 fs² and -200 fs² for the first and the second design problems, respectively (second term in Eq. (2)). As a result, for each design problem one DM was synthesized. The first DM design, named CM1705, contains 22 layers and it has total physical thickness of 6.9 μm . The second one, named CM1708, comprises 26 layers and it has the total thickness of 7.3 μm . Nominal reflectance and GDD curves of CM1705 and CM1708 designs are presented in Fig. 2. The structures of CM1705 and CM1708 designs are shown in Fig. 3(a) and Fig. 4(a), respectively.

The GDD ripples are inevitable in any dispersive mirror. The ripples can broaden/deform the pulse shape and lead to appearance of satellites with initial single pulse [11,16]. The period of the ripples in the spectral domain determines the position of the satellite in the time domain, and the amplitude of these oscillations defines the amount of energy, which transfers into the satellite(s). Until now, there exists no analytical estimations of the amplitude of the GDD ripples, which can lead to deformation of the initial pulse. However, for each designed DM, the model calculations can be performed. In Figs. 2(c)-2(d), the simulated envelopes of the input Fourier-limited pulse and pulse reflected from the designed CM1705 and CM1708 DMs are presented. In the course of the model calculation, it was assumed that the full width of half maximum of the input pulse is 50 THz and the central wavelength is 2500 nm. Despite

the ripples in the GDD, the shape of the reflected pulse is very close to the Fourier-limited one. The duration of input and output pulses are about 24 fs.

The synthesized DMs were fabricated using a Leybold Optics magnetron sputtering Helios plant, with the layer thicknesses controlled using well-calibrated time monitoring [16]. The plant is equipped with two proprietary dual-magnetrons and a plasma source for ion-assisted reactive middle frequency dual magnetron sputtering.

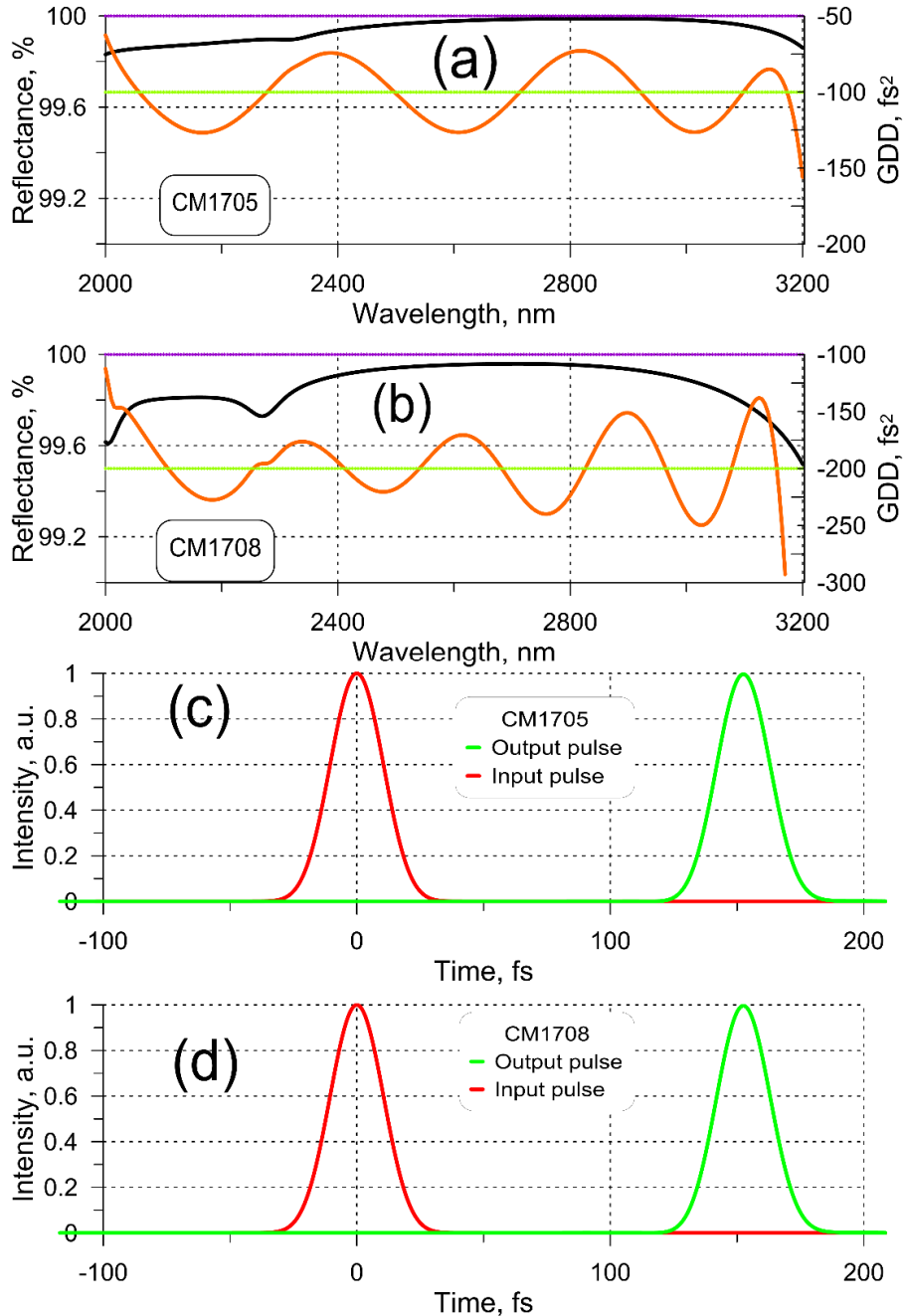


Fig. 2. Nominal spectral performance of the designed DMs and the target spectral characteristics: (a) CM1705, (b) CM1708. Input and output pulse simulations, Output pulse is calculated after four reflections from the CM1705 (c) and from the CM1708 (d).

The magnetrons were optimized for high sputtering rates and high optical layer performance. The system was pumped by turbo-molecular pumps to 1×10^{-6} mbar before deposition. Argon and oxygen were used for both magnetrons. In the magnetron cathodes, Si target was used. The electric power of the Si cathode was 4500W. The gas pressure was 1×10^{-3} mbar during the sputtering process. In the case of SiO₂ layers, oxygen was fed near the targets to oxidize the sputtering films. The distance from the targets to the substrates was 100mm. The purity of the Si target was 99.999%. By changing the electric power applied to the cathode, it was possible to increase or decrease the sputtering rate. We found that the film quality degrades at high rates and good film quality was realized at the rate of around 0.5 nm/s for both materials.

Two samples were fabricated, CM1705 and CM1708 having design structures CM1705 and CM1708, respectively.

3. Experimental data and discussion

After the deposition, reflectance data of CM1705 and CM1708 samples was measured by the URA in the range from 1200 nm to 3100 nm with the wavelength step of 1 nm (see red curves in Fig. 3(b) and Fig. 4(b)), the measurement accuracy is 0.2%. The reflectance data in the high reflection zone from 1900 nm to 3100 nm was taken with a longer acquisition time of 0.5 sec per spectral point in order to achieve measurement accuracy about 0.1%. This experimental data are presented separately in Fig. 3(c) and Fig. 4(c). In order to visualize the performance of the produced DMs, the reflectance data of the mirrors in the high reflection zone is compared with the reflectance data of a gold mirror (see Fig. 3(c) and Fig. 4(c)). It is seen that the reflectance of the produced mirrors exceeds the reflectance of the gold mirror which provides 98.7% reflectivity and can serve as a reference. In Fig. 3(b) and Fig. 4(b), reflectance in the wavelength range from 3000 nm to 5000 nm measured by Fourier transform infrared (FTIR) spectrometer Vertex 70 from Bruker Optics GmbH is shown by blue curves. The measurement accuracy is 0.2%. In Figs. 3(b)–3(c) and Figs. 4(b)–4(c) one can observe the good correspondence between experimental and nominal coating performances. The degradation of reflectance indicated in the range 2600–2900 nm is caused by the OH absorption inevitable even in high-quality optical coatings. In addition, OH vapor in the air absorbs the radiation. The degradation can be observed in the gold mirrors as well. Assuming that each mirror has a reflectance of 99.6%, the total reflectance loss after the six bounces (four bounces at CM1708 and two bounces at CM1705) will be: $(0.996)^6 \cdot 100\% = 97.6\%$. With these six bounces, the GVD of $+1000 \text{ fs}^2$ can be compensated. Actually, GDD after six bounces: $\text{GDD} = -200 \text{ fs}^2 \cdot 4 - 100 \text{ fs}^2 \cdot 2 = -1000 \text{ fs}^2$.

The group delay (GD) experimental values of CM1705 and CM1708 were extracted from the data recorded by a mid-infrared white-light interferometer (WLI) developed in-house [17]. The WLI uses FTIR spectrometer Vertex 70 having an external input which allows one to measure the light from the Michelson-type interferometer described in [17]. The spectral resolution of the WLI is defined by the spectral resolution of the FTIR spectrometer, which in its turn depends on the wavelength. The device records 8000 spectra with a resolution of 10 cm^{-1} . This corresponds to a wavelength resolution of 100 nm at the wavelength of $10 \mu\text{m}$ and to 25 nm at a wavelength of $2 \mu\text{m}$. FTIR spectrometers typically used in the mid-infrared spectral range are less sensitive than visible-near-infrared spectrometers. As a result, the mid-infrared interferograms measured with the WLI are more noisy. For the evaluation of the interferograms acquired by the WLI, a special algorithm was developed [17,18]. The GD values are derived as time points corresponding to the maximum of the interferogram. These points are found by fitting the interferogram with a Gauss-function. The uncertainty in the time axis of this fit is a source of noise in the GD result. The GDD curves are noisier since that are calculated as a derivative of the noisy GD curve. Actually, averaging is applied to smooth the curves, but this unfortunately reduces the spectral resolution. Taking into account

the issues shortly described above, the GDD curves are not presented in the current work. The carefully measured GD data are plotted in Fig. 3(d) and Fig. 4(d). The noise level is about 10-12 fs. In Fig. 3(d) and Fig. 4(d), these values are compared with the theoretical GD curves and the good correspondence is clearly demonstrated.

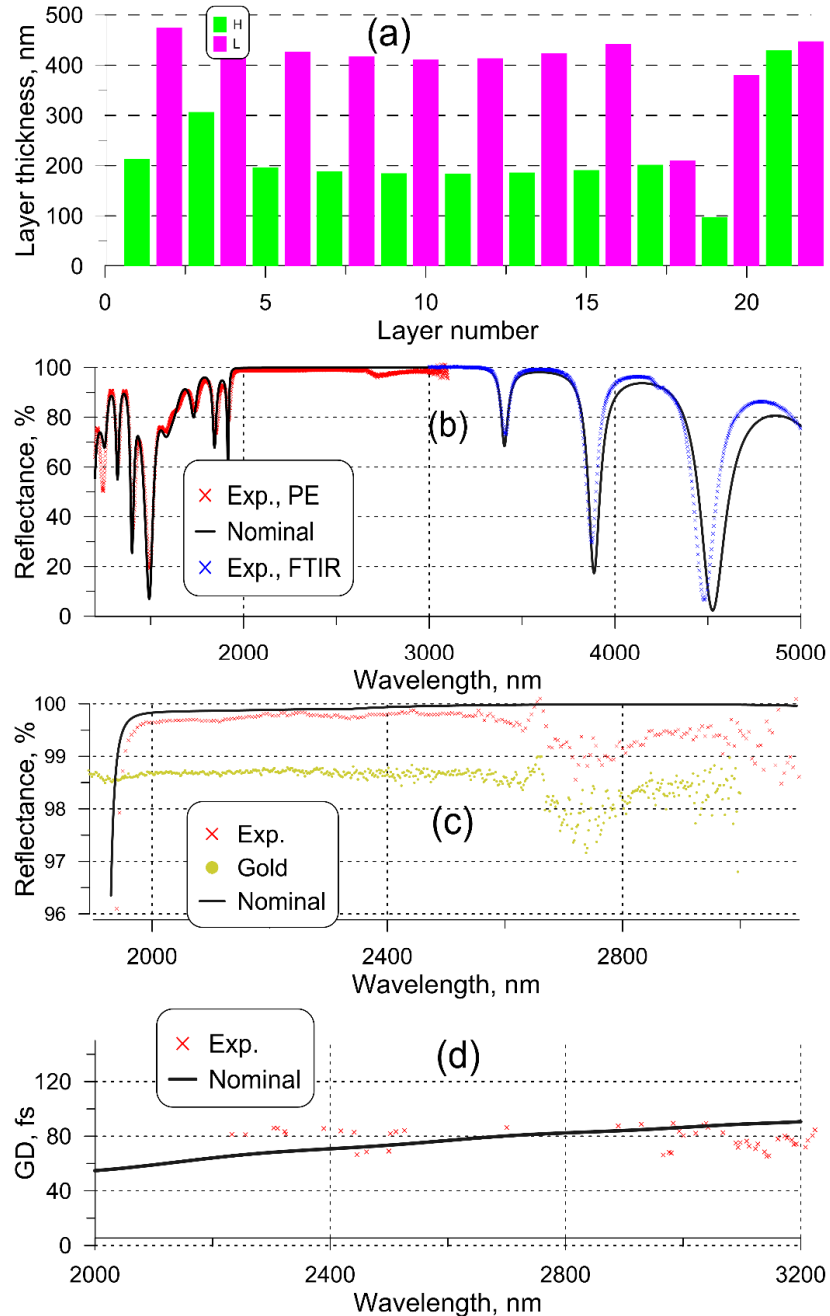


Fig. 3. (a): Structure of CM1705 design; (b): Correspondence between the nominal and experimental reflectance data of CM1705 sample; (c) Comparison of the nominal and experimental reflectance data of CM1705 sample in the high reflectance zone, reflectance of the gold mirror is shown as a reference; (d) Measured and nominal GD of CM1705 sample.

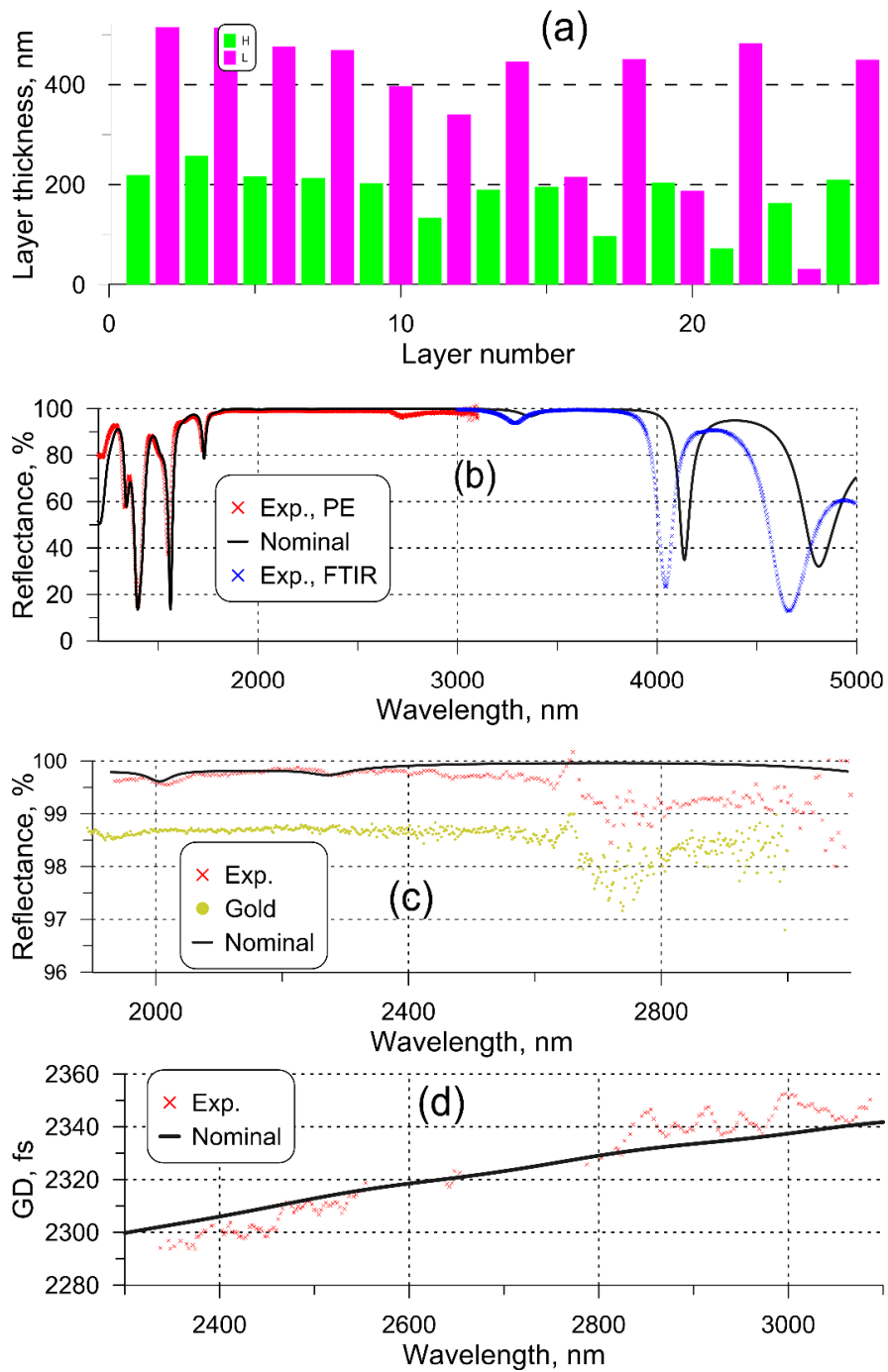


Fig. 4. (a): Structure of CM1708 design; (b): Corresponding between the nominal and experimental reflectance data of CM1708 sample; (c) Comparison of the nominal and experimental reflectance data of CM1708 sample in the high reflectance zone, reflectance of the gold mirror is shown as a reference; (d) Measured and nominal GD of CM1708 sample.

4. Conclusions

Two broadband dispersive mirrors providing the group delay dispersion of -100 fs^2 and -200 fs^2 in the spectral range from 2 to $3.2 \mu\text{m}$ have been successfully designed and produced for the first time. The Si/SiO₂ thin-film material pair has been used in order to provide the high contrast between high and low refractive indices and to achieve high reflectance and specified group delay dispersion in the broadband spectral range. Unprecedented reflectance exceeding 99.6% and proven group delay dispersion in a broadband infrared spectral range allows applications of the produced coatings inside the Cr:ZnS/Cr:ZnSe femtosecond lasers and amplifiers. The new materials pair opens a new horizon in design and production of multilayer optics in 2-4 μm spectral range.

Funding

DFG Cluster of Excellence, “Munich Centre for Advanced Photonics,” (<http://www.munich-photonics.de>). T. Amotchkina received funding from the European Union’s Horizon 2020 research and innovation programme under the Marie Skłodowska-Curie agreement No 657596.

Acknowledgments

The authors thank Prof. F. Krausz for valuable discussion and permanent support of this work.

References

1. V. Pervak, O. Razskazovskaya, I. B. Angelov, K. L. Vodopyanov, and M. Trubetskov, “Dispersive mirror technology for ultrafast lasers in the range 220–4500 nm,” *Adv. Opt. Technol.* **3**, 55–63 (2014).
2. V. Pervak, C. Teisset, A. Sugita, S. Naumov, F. Krausz, and A. Apolonski, “High-dispersive mirrors for femtosecond lasers,” *Opt. Express* **16**(14), 10220–10233 (2008).
3. O. Razskazovskaya, F. Krausz, and V. Pervak, “Multilayer coatings for femto- and attosecond technology,” *Optica* **4**(1), 129–138 (2017).
4. P. Dombi, P. Rác, M. Lenner, V. Pervak, and F. Krausz, “Dispersion management in femtosecond laser oscillators with highly dispersive mirrors,” *Opt. Express* **17**(22), 20598–20604 (2009).
5. E. Fedulova, K. Fritsch, J. Brons, O. Pronin, T. Amotchkina, M. Trubetskov, F. Krausz, and V. Pervak, “Highly-dispersive mirrors reach new levels of dispersion,” *Opt. Express* **23**(11), 13788–13793 (2015).
6. K. Yang, H. Bromberger, H. Ruf, H. Schäfer, J. Neuhaus, T. Dekorsy, C. V.-B. Grimm, M. Helm, K. Biermann, and H. Künzel, “Passively mode-locked Tm,Ho:YAG laser at 2 μm based on saturable absorption of intersubband transitions in quantum wells,” *Opt. Express* **18**(7), 6537–6544 (2010).
7. T. Amotchkina, M. Trubetskov, F. Habel, Y. Pervak, J. Zhang, K. Mak, O. Pronin, F. Krausz, and V. Pervak, “Synthesis, fabrication and characterization of a highly-dispersive mirrors for the 2 μm spectral range,” *Opt. Express* **25**(9), 10234–10240 (2017).
8. S. Mirov, I. Moskalev, S. Vasilyev, V. Smolski, V. Fedorov, D. Martyshkin, J. Peppers, M. Mirov, A. Dergachev, and V. Gapontsev, “Frontiers of mid-IR lasers based on transition metal doped chalcogenides,” *IEEE J. Sel. Top. Quantum Electron.* **24**(5), 1601829 (2018).
9. I. T. Sorokina and E. Sorokin, “Femtosecond Cr²⁺ based lasers,” *IEEE J. Sel. Top. Quantum Electron.* **21**(1), 273–291 (2015).
10. S. Vasilyev, I. Moskalev, M. Mirov, S. Mirov, and V. Gapontsev, “Multi-Watt mid-IR femtosecond polycrystalline Cr²⁺:ZnS and Cr²⁺:ZnSe laser amplifiers with the spectrum spanning 2.0-2.6 μm ,” *Opt. Express* **24**(2), 1616–1623 (2016).
11. G. Steinmeyer, “Femtosecond dispersion compensation with multilayer coatings: toward the optical octave,” *Appl. Opt.* **45**(7), 1484–1490 (2006).
12. H. H. Li, “Refractive index of silicon and germanium and its wavelength and temperature derivatives,” *J. Phys. Chem. Ref. Data* **9**(3), 561–658 (1980).
13. S. A. Furman and A. V. Tikhonravov, *Basics of Optics of Multilayer Systems* (Editions Frontières, 1992).
14. A. V. Tikhonravov, M. K. Trubetskov, and G. W. Debell, “Application of the needle optimization technique to the design of optical coatings,” *Appl. Opt.* **35**(28), 5493–5508 (1996).
15. A. V. Tikhonravov and M. K. Trubetskov, “OptiLayer software,” <http://www.optilayer.com>.
16. V. Pervak, A. V. Tikhonravov, M. K. Trubetskov, S. Naumov, F. Krausz, and A. Apolonski, “1.5-octave chirped mirror for pulse compression down to sub-3 fs,” *Appl. Phys. B* **87**(1), 5–12 (2007).
17. F. Habel, M. Trubetskov, and V. Pervak, “Group delay dispersion measurements in the mid-infrared spectral range of 2-20 μm ,” *Opt. Express* **24**(15), 16705–16710 (2016).
18. T. V. Amotchkina, A. V. Tikhonravov, M. K. Trubetskov, D. Grupe, A. Apolonski, and V. Pervak, “Measurement of group delay of dispersive mirrors with white-light interferometer,” *Appl. Opt.* **48**(5), 949–956 (2009).